DOI: 10.1002/ejic.201100226

Redox-Responsive Rhodocenium [O,O]-, [N,O]-, [N,N]-, and [N,C,N]-Metalloligands

Daniela Eisenstecken,[a] Barbara Enk,[a] Holger Kopacka,[a] Klaus Wurst,[a] Thomas Müller,[b] Florian Pevny,[c] Rainer F. Winter,*[c] and Benno Bildstein*[a]

Keywords: Rhodium / Metallocenes / N ligands / N,O ligands / Electrochemistry

As we have recently shown, the doubly substituted [1,2-O,O]H, [1,2-O,N]H, [1,2-N,N]H, and [1,3-N,N]H pentafulvenes are convenient N/O-functionalized cyclopentadienide (Cp) precursors. Deprotonation of the pentafulvenes by potassium hydride followed by reaction with $[Cp^*RhCl_2]_2$ or $[Cp^*IrCl_2]_2$ gave access to the first functionalized rhodocenium and iridocenium salts that contain two acyl and/or imidoyl substituents. These air-stable compounds represent interesting bis(acyl/imidoyl) or mixed acyl/imidoyl metalloligand systems that combine an axially shielding, electrochemically active metallocene moiety with directly attached, conjugating oxygen and/or nitrogen donor sites. The structural properties of these novel metallocene metalloligands in solution and in the solid state were studied by NMR spectroscopy (^{1}H, ^{13}C, ^{103}Rh) and by single-crystal structure analysis. The electrochemical investigations on complexes **5a**, **6b**, and **7a** showed the effect of the appended functional groups on the potential and on the reversibility of the rhodocenium/rhodocene reduction and provided evidence for the dimerization that followed the reduction. Further redox processes that were due to the heteroatom functions included the stepwise reduction of the 1,2-diketo entity of **5a** and the oxidation of the 1,2-diimino moiety of **7a**.

Introduction

In comparison to the fully developed chemistry of ferrocene and its derivatives, there are surprisingly few reports in the literature of the isoelectronic cobaltocenium, rhodocenium, and iridocenium compounds. The parent, unsubstituted, air-stable group 9 metallocenium salts $(Cp)_2M^+X^-$ (M = Co^{III},[1] Rh^{III},[2] Ir^{III};[2a,3] X = monovalent anion) were synthesized shortly after the discovery of ferrocene,[4] but only scattered studies dealt with such sandwich compounds, as can be inferred from the scarce number of reported compounds within the last 6 decades (Co: > 2000, Rh: > 80, Ir: > 10; for comparison: Fe: > 65000).[5] In general, the importance of the metallocenes (predominantly ferrocenes) stems from their useful properties as the steering ligands in (stereoselective) catalysis, in redox sensing, in supramolecular chemistry, as components of NLO materials, and in biochemical or medicinal applications. These applications usually require metallocenes with appended functional groups, and hence the design of task-specific functionalized metallocenes is a worthwhile endeavour in synthetic organometallic chemistry. The predominance of the ferrocene compounds in this area is due to their ready availability by a wide range of synthetic protocols, the fully reversible ferrocene/ferrocenium redox couple, the biocompatibility of the nontoxic ferrocene moiety, and the low cost of iron in comparison to the expensive platinum group metals, Ru, Os, Rh, and Ir.

In recent work[6] we developed an efficient modular route to pentafulvenes that bear 2/3-acyl/imidoyl-6-hydroxy/amino substituents. These fulvenes are new ambidentate ligands that are capable of forming either κ^2-O/N metal complexes or η^5-cyclopentadienyl sandwich complexes with the acyl/imidoyl substituents, depending on the hardness of the metal electrophile. With "arenophilic", electron-rich, soft, late transition metal moieties like Cp^*Ru^+, the corresponding disubstituted pentamethylruthenocenes[6] are conveniently accessible. This raised the question as to whether this chemistry could be extended to the isoelectronic group 9 metal sandwich complexes of Co^{III}, Rh^{III}, and Ir^{III}.

In this contribution, we report on the first doubly functionalized pentamethylrhodocenium salts, which are based on our recent account on the isoelectronic ruthenocene compounds.[6] In addition, we have shown in one example that the corresponding iridocenium compounds may be synthesized analogously. As mentioned above, only a few functionalized rhodocenium compounds are known. Struc-

[a] Institute of General, Inorganic and Theoretical Chemistry, Faculty of Chemistry and Pharmacy, University of Innsbruck, Innrain 52a, 6020 Innsbruck, Austria
Fax: +43-512-507-2934
E-mail: benno.bildstein@uibk.ac.at
[b] Institute of Organic Chemistry, Faculty of Chemistry and Pharmacy, University of Innsbruck, Innrain 52a, 6020 Innsbruck, Austria
[c] Department of Chemistry, University of Konstanz, Universitätsstraße 10, 78457 Konstanz, Germany
Fax: +49-7531-88-3136
E-mail: rainer.winter@uni-konstanz.de
Supporting information for this article is available on the WWW under http://dx.doi.org/10.1002/ejic.201100226.

turally all of them contain only one substituent per cyclopentadienyl ligand that gives rise to symmetrical 1,1′-disubstituted metallocene cations.[7] In contrast, these new pentamethylrhodocenium compounds bear acyl and/or imidoyl substituents in the 1,2- or 1,3-positions, thereby making useful redox-active metallocene metalloligands accessible that complement the ubiquitous ferrocene compounds. The synthesis as well as the spectroscopic, structural, and electrochemical properties of these compounds are reported and discussed.

Results and Discussion

Synthesis

Firstly, we attempted the synthesis of 1,2-dibenzoyl-1′,2′,3′,4′,5′-pentamethylcobaltocenium iodide by the reaction of deprotonated 2-benzoyl-6-hydroxy-6-phenylpentafulvene[8] with $[Cp^*CoI_2]_2$.[9] No reaction occurred, which indicated the insufficient stability of the desired cobaltocenium species. Electronically, 1,2-diacylcyclopentadienide is an acceptor-substituted cyclopentadienide that forms stable sandwich metallocenes only if the second Cp ligand is able to compensate for the loss of electron density with the combination of the strong Cp–metal bonding. As in the case of Fe^{II}, where no such metallocenes have been observed,[10] the Cp–metal bonds for Co^{III} do not seem to be strong enough to support these acceptor-substituted cyclopentadienides. Therefore, we concluded that only the 4d (Ru,[6] Rh) and 5d (Os,[11] Ir) d^6-metal ions give stable compounds of this type due to their intrinsically stronger carbon–metal bonds in combination with the strongly electron-donating pentamethylcyclopentadienide coligand.

In contrast to the failure with Co^{III}, successful reactions were achieved with Rh^{III} and Ir^{III} (Scheme 1). The deprotonation of the difunctionalized pentafulvenes[6] **1**–**4b** in a tetrahydrofuran solution by using excess potassium hydride (KH) cleanly afforded the intermediate disubstituted cyclopentadienide potassium salts. In our experience, KH is a convenient, non-nucleophilic, selective base that enables clean and complete deprotonations in organometallic chemistry. It is a heterogeneous reaction, and the dihydrogen evolution that occurs during the deprotonation shifts the equilibrium to the product side, and the observation of gas evolution is a convenient way to monitor the course of the reaction. After the deprotonation is complete, the excess KH is easily removed by filtration with the exclusion of air. The subsequent transmetalation with $[Cp^*RhCl_2]_2$ or, in one case, with $[Cp^*IrCl_2]_2$ at ambient temperature over the course of 3–5 d afforded the desired metallocenes **5a**–**8b** in 30–98% isolated yield as yellow to red-brown, air-stable materials. We focused on the rhodocenium salts **5a**, **6a**–**6d**, **7a**,**b**, and **8a**,**b**. The preparation of the iridocenium chloride **5b** was performed mainly to prove the applicability of this synthetic protocol to the 5d-metal Ir. We refrained from synthesizing the other iridocenium salts due to the highly expensive Ir starting materials, but it is generally accepted that Rh^{III} and Ir^{III} show analogous chemical behavior.

The pentamethylmetallocenium salts **5a**,**b**, **7a**,**b**, and **8a**,**b** contain two identical acyl or imidoyl substituents on the second Cp ligand and are therefore achiral, mixed-ligand, symmetrical metallocenes. In contrast, the 1-acyl-2-imidoyl-

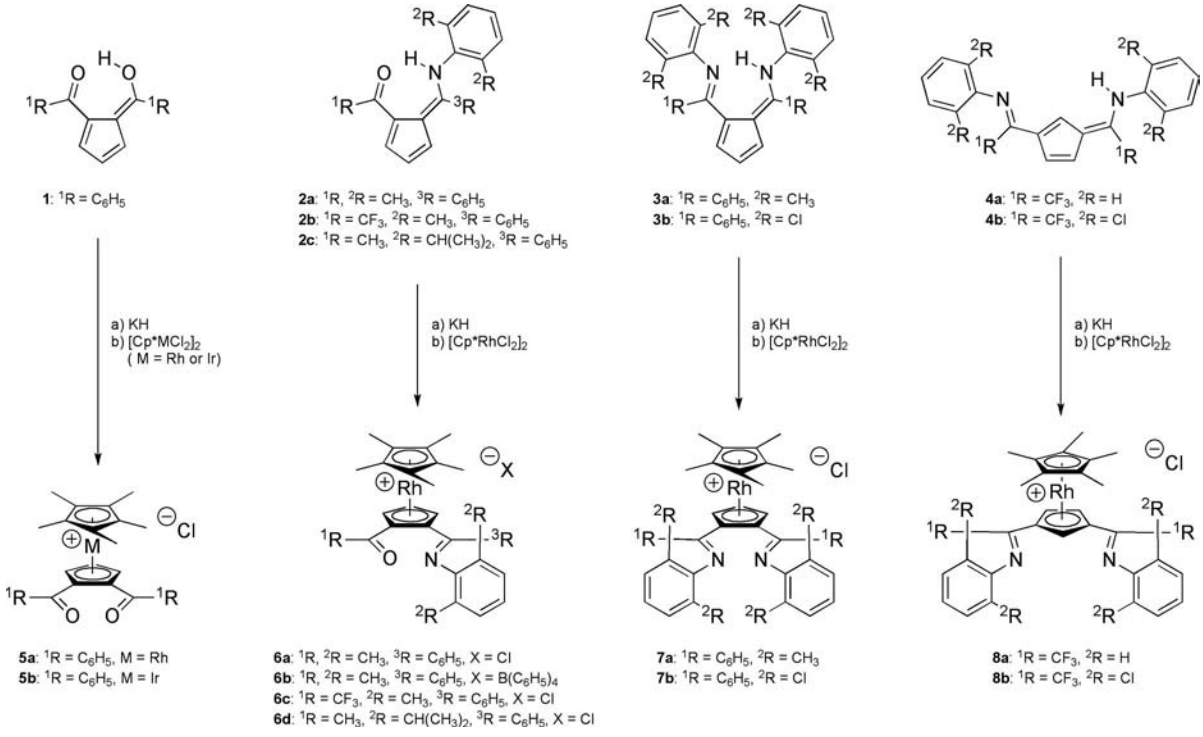

Scheme 1. Synthesis of the doubly functionalized pentamethylrhodocenium/iridocenium salts **5a**–**8b**.

1′,2′,3′,4′,5′-pentamethylrhodocenium salts **6a**–**6d** are racemic, planar-chiral metallocenes due to their unsymmetrical, enantiotopic O,N-disubstituted Cp ligand. For the sake of simplicity, only one of the two enantiomers is shown in Scheme 1. It is likely that optical resolution of these racemic mixtures could have been achieved by fractional crystallization of the diasteromeric salts containing anions from the chiral pool. Rhodocenium salt **6b** was the only compound in this series that had tetraphenylborate as the counterion due to the superior workup and its purification properties (see Experimental Section). The bis(imidoyl)pentamethylrhodocenium chlorides **7a**,**b** and **8a**,**b** both have the same type of substituents but have a different substitution pattern. If a selective *ortho*-metalation at C-2 of the 1,3-bis(imidoyl)-Cp ligand is possible, then **8a**,**b** are precursors to tridentate, monoanionic [N,C,N]-pincer ligands. **7a**,**b**, on the other hand, are bidentate, neutral [N,N]-metalloligands.

Spectroscopic and Structural Properties

In solution, the diagnostic NMR properties of the pentamethylmetallocenium salts **5a**–**8b** are the strong singlet signals of the five isochronic methyl groups of their Cp* ligand that is detected at $\delta \approx 2.0$ (^{1}H) and 10.0 ppm (^{13}C). The acyl and imidoyl functionalities are evident from their ^{13}C NMR signals that are observed at δ = 188–194 (C=O) and 161–169 ppm (C=N). The resolved scalar metal–carbon couplings in the ^{13}C NMR spectra (d, $^1J_{13C\text{-}103Rh}$ = 4–8 Hz) between the central rhodium atom and the carbon atoms of both of the Cp rings allowed the chemical shifts of these carbon atoms to be assigned, except for the iridocenium compound **5b**. The substitution pattern of the 1,2- and 1,3-bis(imidoyl)rhodocenium salts **7a**,**b** and **8a**,**b** is evident from the multiplicity of the ^{1}H NMR signals of the substituted Cp ring hydrogen atoms (**7a**,**b**: t and d; **8a**,**b**: s and s).

In addition to these diagnostic NMR properties, the various alkyl/aryl substituents of **5a**–**8b** gave rise to their expected signals and coupling patterns (see Experimental Section). Whereas the NMR spectra of the non-fluorinated rhodocenium/iridocenium salts are well resolved, less clean and slightly broadened spectra are observed for the trifluoromethylated compounds **6c**, **8a**, and **8b**. We postulate that the most likely reason for this behavior is the increased reactivity of the trifluoromethyl-substituted acyl (**6c**) and imidoyl (**8a**,**b**) functionalities towards water, which stabilizes, to some minor extent, their hemiketal (**6a**/H_2O) and hemiaminal (**8a**,**b**/H_2O) forms, respectively. It is well known that such species can be detected by NMR spectroscopy and/or isolated if electron-withdrawing groups are present.[11] In our case one trifluoromethyl substituent and a cationic rhodocene moiety are present. However, the attempts to shift this equilibrium completely to the hydrated or non-hydrated form by treatment with diluted aqueous acid or base were unsuccessful, and no better resolved NMR spectra were obtained. A second possible reason for the broadened spectra of compounds **6c**, **8a**, and **8b** could be the partial formation of intramolecular O–H–N (**6a**) or intermolecular N–H–N (**8a**,**b**) hydrogen bonds in the presence of water during the workup. In our opinion, this possibility is less likely, because the trifluoromethylated rhodocenium salts are significantly weaker Brønsted bases than the 1,2-bis(imidoyl)rhodocenium chlorides **7a**,**b**, in which a strong intramolecular N–H–N hydrogen bond is to be expected, as analogously demonstrated by the corresponding ruthenocene compounds, where such a species has been unambiguously characterized by a single-crystal structure analysis.[6b]

In addition to standard ^{1}H and ^{13}C NMR spectroscopy, ^{103}Rh NMR spectroscopy[12] is, in principle, applicable for the characterization of **5a**–**8b**, with the exception of the iridocenium salt **5b**. Although the spin 1/2 nuclide ^{103}Rh is 100% abundant, its detection by NMR spectroscopy suffers from its very weak magnetic strength with concomitant very low sensitivity in comparison to other spin 1/2 nuclei. This makes ^{103}Rh one of the most difficult spin 1/2 metal nuclei to measure by transition metal NMR spectroscopy. However, state of the art FT-NMR spectroscopy enables the direct measurement of ^{103}Rh within a reasonable data acquisition time. Because our inhouse NMR spectrometer is unsuitable for such ^{103}Rh NMR measurements, one selected example, **5a**, was measured at an external NMR facility (Bruker Analytical Services, Vienna, Austria). A ^{103}Rh chemical shift of δ = –28.5 ppm was observed [vs. $Rh(acac)_3$ as the external standard], and no other signal was detected within the extremely large ^{103}Rh shift range of over 12000 ppm. This observed chemical shift is extremely deshielded in comparison to the unsubstituted, parent rhodocenium salt, $Cp_2Rh^+Cl^-$ (δ = –10147 ppm).[13,14] A certain degree of deshielding for **5a** was expected due to its two benzoyl acceptor substituents, but such a large difference (over 10000 ppm) cannot be explained by simple substituent effects. At present we are unable to explain this behavior, but it would seem that ^{103}Rh NMR spectroscopy is of limited value for simple structure-related correlations based on the limited data available.

The positive-mode FAB mass spectrometry of the pentamethylrhodocenium/iridocenium salts **5a**–**8b** gave strong signals for their corresponding cations, which thereby further proved the identity of these salts. In addition, the diagnostic stretching vibrations of the carbonyl ($\tilde{\nu}_{C=O}$ = 1644–1686 cm^{-1}) and imine ($\tilde{\nu}_{C=N}$ = 1615–1646 cm^{-1}) functionalities were observed in the IR spectra (see Experimental Section).

The solid-state structures are available for three representatives of the rhodocenium salts. Figures 1, 2, and 3 show the molecular structures of the cations of **5a**, **6b**, and **7a**, respectively; their counterions and the solvent molecules are neglected for clarity. Overall, regular pentamethylmetallocene sandwich structures were observed with one of the acyl/imidoyl substituents roughly coplanar with the substituted Cp ring, whereas the second acyl/imidoyl substituent is approximately orthogonal to the Cp plane. The orthogonal substituents exert some steric hindrance on the upper Cp* ring, which results in a slight deviation from planarity of the Cp and Cp* planes [**5a**: 3.4(1)°; **6b**: 1.8(2)°; **7a**:

8.9(6)°]. The average distances from the Rh center to the Cp* carbon atoms are shorter by approximately 3 pm in comparison to those of the Cp carbon atoms. This reflects the higher electron density of the Cp* ligand and the slightly reduced metal–ligand bonding of the acceptor-substituted Cp ligand. In the structures with imidoyl groups (**6b**, **7a**), the *N*-aryl groups are strongly tilted with respect to the C=N π-plane, which is due to steric hindrance by their 2,6-substituents. At first sight one might think that these [O,O], [N,O], and [N,N] metalloligands are incapable of forming chelate metal complexes due to their strongly tilted donor groups; however, we attribute their different orientation mainly to the crystal-packing forces and expected the normal coordination chemistry for these ligands.

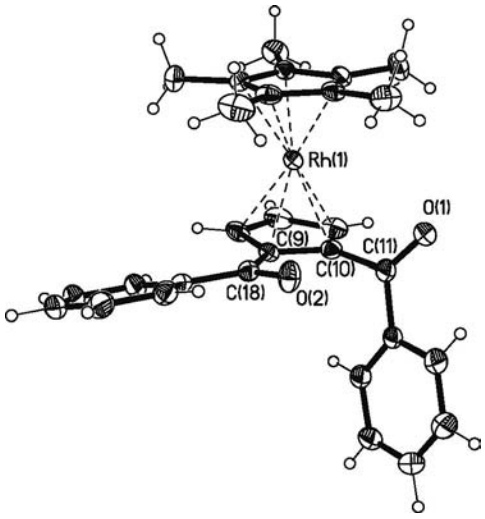

Figure 1. Molecular structure of the cation of **5a**; the solvent molecules (H_2O) are omitted for clarity. Selected bond lengths [Å]: C(11)–O(1) 1.213(2), C(18)–O(2) 1.220(2).

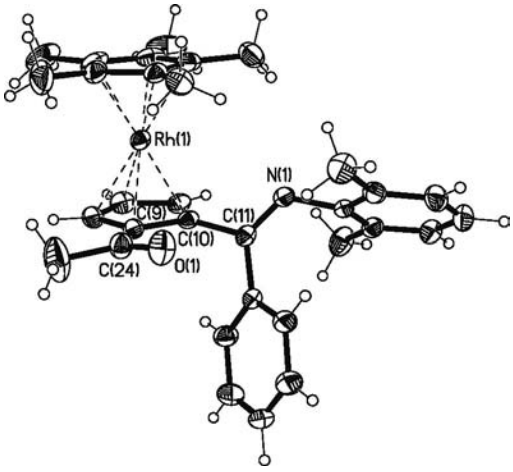

Figure 2. Molecular structure of the cation of **6b**; the solvent molecules (CH_2Cl_2) are omitted for clarity. Selected bond lengths [Å]: C(11)–N(1) 1.272(3), C(24)–O(1) 1.208(3).

As shown recently in one case of the isoelectronic [N,N] ruthenocenes,[6b] intramolecular chelate formation is possible.

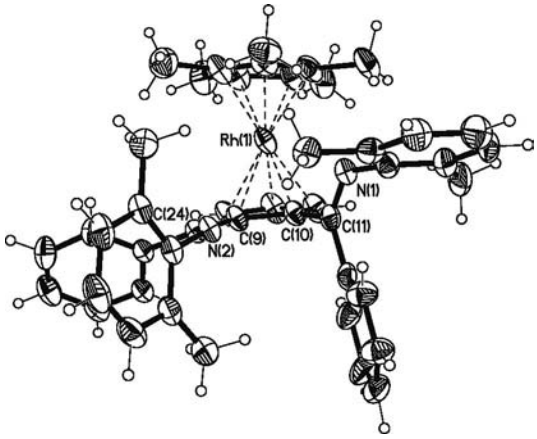

Figure 3. Molecular structure of the cation of **7a**; the solvent molecules (CH_2Cl_2) are omitted for clarity. Selected bond lengths [Å]: C(11)–N(1) 1.278(8), C(24)–N(2) 1.280(8).

Electrochemical Properties

A possible advantage of the metallocene metalloligands over conventional diketone, imino ketone, or diimine chelates is the redox activity associated with the metallocene scaffolds. As an initial test of the redox properties of these systems, one representative from each of the complex series **5**, **6**, and **7**, namely **5a**, **6b**, and **7a**, was chosen for the electrochemical studies. The parent rhodocene, like other metallocenes of the heavier 4d and 5d congeners of the group 6–9 metals, is a chemically reactive species and exists only at low temperatures in a true sandwich structure. The warming of the parent rhodocene caused rapid dimerization to a bis(η^5-cyclopentadienyl)(μ-η^4:η^4-dihydrofulvalene)dirhodium structure where both rhodium atoms attain their 18 valence electron configuration. This dimerization can be reversed at high temperatures by means of scission of the dihydrofulvalene linkage.[15] The high chemical reactivity of the rhodocenes was also indicated by the peculiarities observed in the electrochemical experiments on the reduction of the rhodocenium cations. The parent rhodocenium was reduced at –1.81 V in CH_3CN/Bu_4NPF_6 to give rhodocene, the half-life of which was estimated to be 2 s at room temperature from the ratio of the reverse and forward peak currents. A small anodic peak at –0.9 V on the reverse scan indicated the formation of the fulvalene-bridged dimer, which was prepared and identified by bulk electrolysis.[16] The replacement by one or two of the Cp rings with sterically more demanding and more electron-rich Cp* ligands (Cp* = η^5-C_5Me_5) caused a shift in the first reduction potential to –2.03 or –2.38 V in THF/Bu_4NPF_6.[17] The potentials of the original references were transformed to the $Cp_2Fe^{0/+}$ scale by the conversion factors given by Geiger and Connelly.[18] The corresponding methylated rhodocenes proved no less reactive than their unmethylated parent, but

they followed different reaction pathways. Cp*CpRh rapidly transformed to the "mixed" dihydrofulvalene CpRh(μ-η^4:η^4-C_5Me_5–C_5H_5)RhCp*. The dimerization of Cp^*_2Rh was, however, hampered by the permethylation of both of the rings such that the diene complex Cp*(η^4-C_5Me_5H)Rh formed by hydrogen abstraction from the solvent. The rhodocene derived from the indenyl derivative, Cp*(η^5-C_9H_7)Rh^+, nevertheless proved to be completely stable towards dimerization and hydrogen abstraction, possibly because of the facile "indenyl shift", and gave Cp*(η^3-C_9H_7)Rh with a 17 valence electron configuration at the metal atom.

The 1,2-diketo-, 1,2-ketoimine-, and 1,2-diimine-functionalized complexes **5a**, **6b**, and **7a** followed the same general behavior as the other Cp*CpRh$^+$ cations, but the different substituents had major effects on the redox potentials and reactivities of the resulting rhodocenes. All of these rhodocenium ions underwent a primary reduction process in CH_2Cl_2/Bu_4NPF_6 (0.1 M). Its one-electron nature was ascertained by comparison of the forward peak currents to those of the ferrocene or decamethylferrocene standard (Table 1).

Table 1. Redox potentials [V] of the rhodocenium salts **5a**, **6b**, and **7a**.

	$E_{1/2}{}^{+/0}$	$E_{p,follow}$	Other waves
5a	–1.59	–0.96	–2.04, –2.29[a], 0.73[b]
6b	–1.805	–1.20	–0.36[c]
7a	–1.80	–1.14, –1.23	0.73[b], 0.99[d]

[a] Half-wave potentials for the stepwise reduction of the 1,2-diketo functionality at v = 0.1 V/s, T = –70 °C. [b] Peak potential for the chloride oxidation. [c] Peak potential of the Ph_4B^- oxidation. [d] Half-wave potential for the 1,2-diimine oxidation at v = 0.1 V/s, T = –70 °C.

Not surprisingly, the diketo-functionalized **5a** displayed the least negative reduction potential of –1.59 V (–1.60 V at –70 °C) and also the highest degree of chemical reversibility for the +/0 wave (see Figure 4a). Thus, at room temperature, a small cathodic peak at –0.96 V (peak C in Figure 4a) is seen at the intermediate sweep rates (v) but not at the low v (where the follow product, which is not present in the bulk solution, escaped by means of diffusive losses), or at the high v (where the follow reaction was suppressed), or at any sweep rate at –70 °C. The substitution of one or both of the keto functions by imino groups caused a distinct shift in $E_{1/2}$ to more negative values of about –1.80 V (Table 1). Although complexes **6b** and **7a** have very similar redox potentials, they dramatically differ in the stability of the corresponding rhodocene. Thus, whereas the rhodocene associated with **6b** is only slightly more reactive than that formed from **5a**, the rhodocene associated with **7a** is much more reactive so that cooling to –70 °C and sweep rates of $>$ 0.2 V/s were required in order to observe the anodic counterpeak of the **7a**/**7a**$^-$ couple (see Figure 4b, c).

As for **5a** and other rhodocenium ions, traversing the reduction wave also caused one (**6b**) or two (**7a**) new anodic peaks to appear on the backward scan. The potential of these anodic peaks was more than 200 mV more negative

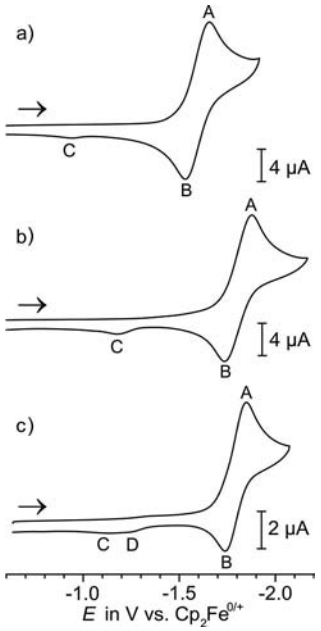

Figure 4. Cyclic voltammetry of complex (a) **5a** (at r.t.), (b) **6b** (at r.t.), and (c) **7a** (at –70 °C, 0.1 M NBu_4PF_4/CH_2Cl_2) at v = 0.4 V/s.

than that obtained for **5a** (peak C in Figure 4b, c; see Table 1). It was clear from the hold-scan experiments, which had different delays starting from potentials that were more negative than the rhodocenium/rhodocene couple, and from the comparative cathodic scans, where the sweep was clipped before traversing the reduction wave, that this peak is due to a product formed from the rhodocene. The scans that were performed at various concentrations of the rhodocenium ions, but under otherwise identical conditions, showed that when the analyte concentration was increased the chemical reversibility decreased, which was measured by the peak current ratios of the reoxidation peak B and the forward reduction peak A, and the amount of follow product that formed increased, which was measured by the ratio of the current of peak C to that of peak A. This pointed to a reaction of higher order in rhodocene concentration, which is in line with the formation of a dimer. Peak D, which was only observed in the case of **7a** (the most bulky of all of the rhodocenium ions), did not seem to show concentration dependence and may thus be due to the diene complex that forms as a result of hydrogen abstraction (see Figures S1–S6 of the Supporting Information).

At more negative potentials, complex **5a** showed two more reduction waves in addition to the rhodocenium/rhodocene couple. Owing to the rapid degradation of these higher reduced forms and the somewhat sluggish electron-transfer kinetics that led to severe wave broadening at the higher sweep rates, these waves were best observed at –70 °C and at low sweep rates (see Figure 5). They are most probably associated with the stepwise reduction of the 1,2-diketocyclopentadienide to the keto enolate and then the 1,2-dimethylenediolate forms, possibly with a hapticity change of the reduced cyclopentadienide ligands as sketched in Scheme 2. No further reductions were observed for **6b** and

7a within the potential window of the CH_2Cl_2/Bu_4NPF_6 supporting electrolyte. During the oxidative scans the complex salts **5a**, **6b**, and **7a** also displayed the typical irreversible oxidation waves of the corresponding counterions with the anodic peak of the Cl^-/Cl_2 couple near +0.73 V and the peak of the $Ph_4B^- \rightarrow Ph_3B$ + 1/2 biphenyl process at +0.36 V. Only in the case of **7a**, the most electron-rich metallocene metalloligand, was an additional oxidation wave observed. Whereas the process was completely irreversible at room temperature, it developed into a quasireversible feature at $E_{1/2}$ = +0.99 V at –70 °C (Figure S7 of the Supporting Information). It was thus attributed to the oxidation of the bis(imine) functionality.

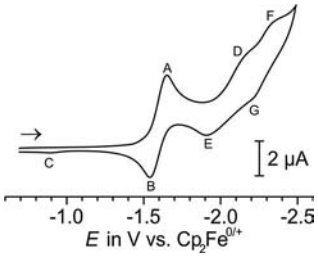

Figure 5. Cyclic voltammetry of complex **5a** (0.1 M Bu_4NPF_4/CH_2Cl_2, –70 °C) at v = 0.1 V/s.

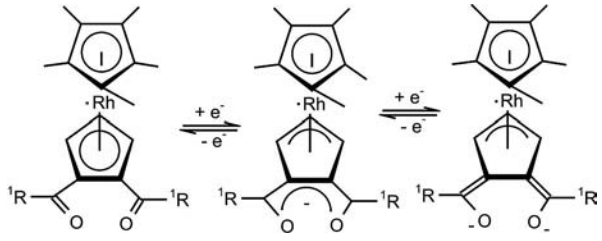

Scheme 2. Ligand-centered reductions of complex **5a**.

Conclusions

The readily available pentafulvenes that bear one acyl or imidoyl substituent and one further tautomerized acyl or imidoyl group are convenient precursors for doubly N/O-substituted cyclopentadienide ligands. After deprotonation of the ligand precursors by potassium hydride, reaction with an arenophilic pentamethylcyclopentadienylrhodium(III) moiety yielded the first rhodocenium salts with two acyl/imidoyl functionalities on one cyclopentadienyl ligand. It was shown in one case that analogous chemistry is possible with Ir^{III}, starting from the respective pentamethylcyclopentadienyliridium(III) chloride. These air-stable salts are new "metalloligands" that are composed of an electrochemically responsive pentamethylrhodocenium core and two directly attached ketone or imine functionalities. Four different families of compounds were prepared. Firstly, the 1,2-diacyl derivatives, which are interesting diketones for further chemical transformations by condensation reactions with functionalized amines, were synthesized. Secondly, the 1-acyl-2-imidoyl derivatives, which are racemic, planar-chiral imino ketones that are new chiral [N,O]-ligand systems and are useful precursors for higher denticity ligand systems by condensation of their acyl functionality, were prepared. Thirdly, the 1,2-bis(imidoyl) derivatives, which are interesting diimine ligands whose steric protection can be tuned through the appended *N*-aryl substituents, were produced. And finally, the 1,3-bis(imidoyl) derivatives, which are regioisomers of the former family of compounds and are interesting precursors to the novel metallocene [N,C,N]-pincer ligand systems, were prepared.

These rhodocenium salts behave as regular metallocenes with the expected spectroscopic and structural properties as was shown by ^1H and ^{13}C NMR spectroscopy, IR spectroscopy, and FAB mass spectrometry. Due to the presence of the spin 1/2 and 100% abundant ^{103}Rh nucleus, diagnostic $^1J(^{13}C\text{-}^{103}Rh)$ couplings were observed in their ^{13}C NMR spectra. The single-crystal structure analyses of the three representatives showed more or less regular metallocenes with strongly tilted acyl/imidoyl substituents. The electrochemical investigations showed that the rhodocenium ions may be reduced to the corresponding rhodocenes and that the reduction potentials and the chemical reactivity of the thus formed rhodocenes depend on the substituents. We expect that the electrochemical properties are further modified by metal coordination of the donor functions and that redox chemistry can be used to alter the electron-donating properties of these metallocene metalloligands.

In future work we plan to exploit the coordination chemistry of these new N/O-ligand systems. We are especially interested in the steric and electronic influence of the directly attached pentamethylrhodocenium moiety on the reactivity, physical properties, and catalytic applications of the metal complexes of these new metalloligands.

Experimental Section

General Considerations: All of the reactions and manipulations of the air- and/or moisture-sensitive compounds were carried out under dry argon by using standard Schlenk techniques. The solvent tetrahydrofuran (THF) was dried with and distilled from Na under argon prior to use. The chemicals were commercially obtained and used as received. The fulvenes **1**–**4b** were prepared as published recently.[6] The NMR spectra were recorded with a Bruker Avance DPX 300 (300 MHz) spectrometer (^1H, ^{13}C) or with a Bruker Avance III 400 (400 MHz) spectrometer (^{103}Rh); the chemical shifts are reported in ppm relative to $Si(CH_3)_4$ (^1H, ^{13}C) or $Rh(acac)_3$ (^{103}Rh).[14] The IR spectra were recorded with a THERMO Nicolet 5700 ATR-FTIR spectrometer. The melting points were measured with a Leica Galen Kofler microscope. The mass spectra were recorded with a Finnegan MAT 95 mass spectrometer.

Representative Procedure for the Synthesis of 5a–8b: A Schlenk tube was charged under argon with pentafulvene **1**–**4b** (0.81 mmol), dry THF (20 mL) and a stirring bar. After the solution had been cooled to 0 °C, an excess of potassium hydride (approximately 100 mg, 2.49 mmol) was added in one portion with the exclusion of air. The external cooling bath was removed, and the stirred mixture was warmed to ambient temperature. During this period dihydrogen evolution was observed with the concomitant darkening of the solution, which indicated the formation of the potassium salt of

the deprotonated functionalized fulvene. After the mixture had been stirred at room temperature overnight, the excess, unreacted potassium hydride was filtered off, and $[Cp^*RhCl_2]_2$ (250 mg, 0.40 mmol) was added. The solution was stirred under argon at room temperature for 4 d. The volatile materials were removed by means of a vacuum line, the residue was exposed to air and then hydrolyzed by the addition of water. The organic materials were extracted at neutral pH with dichloromethane (3×), and the organic layers were combined and dried with extraction with brine and the addition of Na_2SO_4. The volatile materials were removed with a rotary evaporator. The crude product mixture was dissolved in dichloromethane (3 mL) and chromatographed through a short column of silica. Elution with dichloromethane afforded the unreacted ligand precursor, and elution with methanol afforded the pure product as a yellow to red-brown microcrystalline solid after solvent removal.

1,2-Dibenzoyl-1′,2′,3′,4′,5′-pentamethylrhodocenium Chloride (5a): Starting materials: 2-benzoyl-6-hydroxy-6-phenylpentafulvene (**1**) (222 mg, 0.81 mmol) and $[Cp^*RhCl_2]_2$ (250 mg, 0.40 mmol). Yield: 353 mg (80%). M.p. 135 °C. ^{1}H NMR (300 MHz, CD_2Cl_2, 298 K): δ = 2.04 (s, 15 H, Cp*CH_3), 6.22 (d, 2 H, Cp*H*), 6.73 (unresolved t, 1 H, Cp*H*), 7.42 (t, 4 H, *o*-Ph*H*), 7.56 (t, 2 H, *p*-Ph*H*), 7.77 (d, 4 H, *m*-Ph*H*) ppm. ^{13}C NMR (300 MHz, CD_2Cl_2, 298 K): δ = 10.0 (Cp*CH_3), 91.7 [d, $^1J(^{103}Rh\text{-}^{13}C)$ = 6.2 Hz, Cp], 92.6 [d, $^1J(^{103}Rh\text{-}^{13}C)$ = 6.2 Hz, Cp*], 103.8 [d, $^1J(^{103}Rh\text{-}^{13}C)$ = 8.2 Hz, Cp], 129.0 (*o*-Ph), 129.2 (*m*-Ph), 134.4 (*p*-Ph), 136.3 (Ph), 188.7 (*C*=O) ppm. ^{103}Rh NMR (400 MHz, CD_2Cl_2, 300 K): δ = –28.5 ppm. MS (FAB pos): *m*/*z* = 511.08 (M^+ of cation). IR (ATR): $\tilde{\nu}$ = 671 (m), 695 (s), 716 (s), 740 (s), 839 (m), 856 (s), 931 (s), 1024 (m), 1174 (m), 1249 (s), 1338 (s), 1379 (m), 1448 (m), 1468 (w), 1575 (m), 1588 (m), 1644 (s, C=O), 2914 (w), 3052 (w), 3350 (m) cm^{-1}. $C_{29}H_{28}ClO_2Rh$ (546.90): calcd. C 63.69, H 5.16; found C 63.90, H 5.18. Single-crystal structure analysis: Table 2, Figure 1.

1,2-Dibenzoyl-1′,2′,3′,4′,5′-pentamethyliridocenium Chloride (5b): Starting materials: 2-benzoyl-6-hydroxy-6-phenylpentafulvene (**1**) (362 mg, 1.32 mmol) and $[Cp^*IrCl_2]_2$ (500 mg, 0.63 mmol). Yield: 213 mg (30%). ^{1}H NMR (300 MHz, $CDCl_3$, 298 K): δ = 2.07 (s, 15 H, Cp*CH_3), 6.15 (s, 2 H, Cp*H*), 6.95 (s, 1 H, Cp*H*), 7.37–7.42 (m, 4 H, *o*-Ph*H*), 7.51–7.53 (m, 2 H, *p*-Ph*H*), 7.74–7.77 (m, 4 H, *m*-Ph*H*) ppm. ^{13}C NMR (300 MHz, $CDCl_3$, 298 K): δ = 10.1 (Cp*CH_3), 84.6 (Cp), 86.9 (Cp), 97.1 (Cp*), 128.8–129.4 (br. signal, Ph), 134.6 (Ph), 136.0 (Ph), 188.4 (*C*=O) ppm. MS (FAB pos): *m*/*z* = 600.93 (M^+ of cation). IR (ATR): $\tilde{\nu}$ = 696 (s), 714 (m), 796 (w), 858 (m), 938 (m), 1023 (m), 1072 (m), 1246 (m), 1335 (m), 1375 (w), 1446 (m), 1575 (m), 1595 (s), 1650 (s, C=O), 1722 (w), 2910 (w), 2954 (w), 3373 (m) cm^{-1}. $C_{29}H_{28}ClIrO_2$ (636.21): calcd. C 54.75, H 4.44; found C 54.88, H 4.45.

1-(2-{[(2,6-Dimethylphenyl)imino](phenyl)methyl}-1′,2′,3′,4′,5′-pentamethylrhodocen-1-yl)ethanone Chloride (6a)/Tetraphenylborate (6b): Starting materials: 1-(5-{1-[(2,6-dimethylphenyl)amino]-1-phenylmethylene}cyclopenta-1,3-dien-1-yl)ethanone (**2a**) (511 mg, 1.62 mmol) and $[Cp^*RhCl_2]_2$ (500 mg, 0.81 mmol). Yield: 940 mg (99%) of **6a**. M.p. 115 °C. For analytical purposes **6a** was converted into **6b** by anion exchange in methanolic solution. Spectral data for **6b**: ^{1}H NMR (300 MHz, CD_2Cl_2, 298 K): δ = 1.87 (s, 3 H, CH_3), 1.96 (s, 15 H, Cp*CH_3), 2.11 (s, 3 H, CH_3), 2.36 [s, 3 H, C(O)CH_3], 5.03 (t, 1 H, Cp*H*), 5.24 (d, 1 H, Cp*H*), 5.57 (d, 1 H, Cp*H*), 6.87–6.91 (m, 6 H, Ph*H*), 6.99–7.06 (m, 11 H, Ph*H*), 7.19 (t, 2 H, Ph*H*), 7.28 (d, 1 H, Ph*H*), 7.35–7.36 (unresolved m, 8 H, Ph*H*) ppm. ^{13}C NMR (300 MHz, CD_2Cl_2, 298 K): δ = 10.6 (Cp*CH_3), 18.7 [C(O)CH_3], 28.9 (CH_3), 88.8 [d, $^1J(^{103}Rh\text{-}^{13}C)$ = 6.5 Hz, Cp], 89.5 [d, $^1J(^{103}Rh\text{-}^{13}C)$ = 6.6 Hz, Cp], 91.2 [d, $^1J(^{103}Rh\text{-}^{13}C)$ = 6.2 Hz, Cp], 97.9 [d, $^1J(^{103}Rh\text{-}^{13}C)$ = 6.5 Hz, Cp], 103.5 [d, $^1J(^{103}Rh\text{-}^{13}C)$ = 8.4 Hz, Cp*], 109.3 [d, $^1J(^{103}Rh\text{-}^{13}C)$ = 6.8 Hz, Cp], 122.1 (Ph), 123.9 (Ph), 125.9 [q, $^3J(^{11}B\text{-}^{13}C)$ = 2.2 Hz, Ph of tetraphenylborate], 127.0 (Ph), 127.9 (Ph), 128.4 (Ph), 128.5 (Ph), 130.6 (Ph), 135.4 (Ph), 136.3 (Ph), 147.6 (Ph), 160.9 (*C*=N), 164.2 [q, $^1J(^{11}B\text{-}^{13}C)$ = 49.1 Hz, Ph of tetraphenylborate], 192.8 (*C*=O) ppm. MS (FAB pos): *m*/*z* = 552.12 (M^+ of cation). IR (ATR): $\tilde{\nu}$ = 610 (m), 695 (s), 706 (s), 733 (s), 840 (m), 903 (m), 1019 (w), 1148 (w), 1210 (w), 1263 (m), 1343 (w), 1379 (w), 1419 (m), 1450 (m), 1472 (m), 1579 (w), 1637 (m, C=N), 1686 (m, C=O), 2852 (w), 2914 (w), 2985 (w), 3052 (w), 3092 (w) cm^{-1}. $C_{56}H_{55}BNORh$ (871.78): calcd. C 77.15, H 6.36, N 1.61; found C 77.22, H 6.39, N 1.59. Single-crystal structure analysis of **6b**: Table 2, Figure 2.

1-(2-{[(2,6-Dimethylphenyl)imino](phenyl)methyl}-1′,2′,3′,4′,5′-pentamethylrhodocen-1-yl)-2,2,2-trifluoroethanone Chloride (6c): Starting materials: 1-(5-{1-[(2,6-dimethylphenyl)amino]-1-phenylmethylene}cyclopenta-1,3-dien-1-yl)-2,2,2-trifluoroethanone (**2b**) (299 mg, 0.81 mmol) and $[Cp^*RhCl_2]_2$ (250 mg, 0.40 mmol). Yield: 444 mg (86%). ^{1}H NMR (300 MHz, CD_2Cl_2, 298 K): δ = 1.25 (br. s, 3 H, CH_3), 1.61 (br. s, 3 H, CH_3), 2.23 (br. s, 15 H, Cp*CH_3), 4.21 (q, 1 H, O*H*), 4.67 (br. s, 3 H, Cp*H*), 6.70–7.07 (br. m, 6 H, Ph*H*), 7.51–7.71 (br. m, 2 H, Ph*H*) ppm. ^{13}C NMR (300 MHz, CD_2Cl_2, 298 K): δ = 11.1 (Cp*CH_3), 11.2 (Cp*CH_3), 14.1 (CH_3), 68.3 (Cp), 103.8 (br., Cp), 127.0, 128.1, 128.2, 128.3, 128.6, 128.8, 129.0, 129.4, 131.2 (Ph), 167.9 (*C*=N) ppm. MS (FAB pos): *m*/*z* = 606.08 (M^+ of cation). IR (ATR): $\tilde{\nu}$ = 705 (m), 769 (m), 871 (m), 952 (w), 1023 (m), 1130 (m), 1169 (s), 1214 (m), 1290 (w), 1335 (w), 1375 (w), 1446 (m), 1468 (m), 1584 (m), 1606 (m), 1722 (w), 2856 (w), 2919 (w), 3034 (w), 3355 (w) cm^{-1}. $C_{32}H_{32}ClF_3NORh$ (641.97): calcd. C 59.87, H 5.02, N 2.18; found C 60.01, H 5.00, N 2.15.

1-(2-{[(2,6-Diisopropylphenyl)imino](phenyl)methyl}-1′,2′,3′,4′,5′-pentamethylrhodocen-1-yl)ethanone Chloride (6d): Starting materials: 1-(5-{1-[(2,6-diisopropylphenyl)amino]-1-phenylmethylene}-cyclopenta-1,3-dien-1-yl)ethanone (**2c**) (240 mg, 0.81 mmol) and $[Cp^*RhCl_2]_2$ (200 mg, 0.32 mmol). Yield: 324 mg (78%). ^{1}H NMR (300 MHz, CD_2Cl_2, 298 K): δ = 0.77 [d, 3 H, CH(CH_3)$_2$], 1.07 [d, 3 H, CH(CH_3)$_2$], 1.21 [dd, 6 H, CH(CH_3)$_2$], 2.14 (s, 15 H, Cp*CH_3), 2.39 [s, 3 H, C(O)CH_3], 2.59 [sept, 1 H, C*H*(CH$_3$)$_2$], 3.22 [sept, 1 H, C*H*(CH$_3$)$_2$], 5.88 (br. s, 1 H, Cp*H*), 6.38 (br. s, 1 H, Cp*H*), 6.82 (br. s, 1 H, Cp*H*), 6.95–7.05 (m, 4 H, Ph*H*), 7.10–7.15 (m, 4 H, Ph*H*) ppm. ^{13}C NMR (300 MHz, CD_2Cl_2, 298 K): δ = 10.6 (Cp*CH_3), 21.9 [CH(CH_3)$_2$], 23.2 [CH(CH_3)$_2$], 24.2 [CH(CH_3)$_2$], 25.3 [CH(CH_3)$_2$], 28.1 [CH(CH$_3$)$_2$], 28.3 [CH(CH$_3$)$_2$], 29.5 (CH_3), 91.0 [d, $^1J(^{103}Rh\text{-}^{13}C)$ = 4.3 Hz, Cp], 91.5 [d, $^1J(^{103}Rh\text{-}^{13}C)$ = 6.1 Hz, Cp*], 95.2 (unresolved d, Cp), 123.6, 123.8, 124.6, 128.2, 128.7, 130.4, 134.7, 135.1, 137.4, 145.2 (Ph), 161.1 (*C*=N), 194.1 (*C*=O) ppm. MS (ESI pos): *m*/*z* = 608.18 (M^+ of cation). IR (ATR): $\tilde{\nu}$ = 696 (s), 762 (s), 902.8 (w), 952 (w), 1026 (m), 1152 (w), 1232 (m), 1343 (m), 1357 (m), 1379 (m), 1456 (s), 1584 (w), 1633 (m, C=N), 1682 (s, C=O), 2861 (w), 2914 (w), 2959 (m), 3057 (w), 3373 (m) cm^{-1}. $C_{36}H_{43}ClNORh$ (644.11): calcd. C 67.13, H 6.73, N 2.17; found C 67.33, H 6.75, N 2.15.

1,2-Bis{[(2,6-dimethylphenyl)imino](phenyl)methyl}-1′,2′,3′,4′,5′-pentamethylrhodocenium Chloride (7a): Starting materials: 2,6-dimethyl-*N*-(1-{5-[1-(2,6-dimethylphenyl)amino-1-phenylmethylene]-cyclopenta-1,3-dien-1-yl}-1-phenylmethylene)aniline (**3a**) (778 mg, 1.62 mmol) and $[Cp^*RhCl_2]_2$ (500 mg, 0.81 mmol). Yield: 535 mg (44%). ^{1}H NMR (300 MHz, CD_2Cl_2, 298 K): δ = 1.48 (s, 6 H, CH_3), 2.06 (s, 6 H, CH_3), 2.22 (s, 15 H, Cp*CH_3), 5.31 (t, 1 H, Cp*H*), 5.85 (d, 2 H, Cp*H*), 6.75 (d, 4 H, Ph*H*), 6.85–6.88 (m, 2 H, Ph*H*), 6.95–6.98 (m, 4 H, Ph*H*), 7.12 (t, 4 H, Ph*H*), 7.23 (t, 2 H,

Ph*H*) ppm. ^{13}C NMR (300 MHz, CD_2Cl_2, 298 K): δ = 11.3 (Cp*CH_3), 17.9 (CH_3), 19.2 (CH_3), 90.4 [d, $^1J(^{103}Rh\text{-}^{13}C)$ = 7.2 Hz, Cp], 91.5 [d, $^1J(^{103}Rh\text{-}^{13}C)$ = 6.8 Hz, Cp], 103.4 [d, $^1J(^{103}Rh\text{-}^{13}C)$ = 8.1 Hz, Cp*], 105.5 [d, $^1J(^{103}Rh\text{-}^{13}C)$ = 6.2 Hz, Cp], 123.5, 124.8, 126.2, 128.0, 128.4, 130.3, 135.7, 148.1 (Ph), 161.7 (*C*=N) ppm. MS (FAB pos): *m*/*z* = 717.30 (M^+ of cation). IR (ATR): $\tilde{\nu}$ = 693 (s), 720 (s), 760 (s), 885 (m), 956 (w), 1019 (m), 1085 (m), 1157 (w), 1219 (w), 1246 (m), 1343 (m), 1379 (w), 1437 (m), 1468 (m), 1588 (m), 1610 (m), 1628 (m, C=N), 2848 (w), 2914 (w), 2963 (w), 3057 (w), 3364 (m) cm^{-1}. $C_{45}H_{46}ClN_2Rh$ (753.24): calcd. C 71.76, H 6.16, N 3.72; found C 71.85, H 6.19, N 3.74. Single-crystal structure analysis: Table 2, Figure 3.

1,2-Bis{[(2,6-dichlorophenyl)imino](phenyl)methyl}-1′,2′,3′,4′,5′-pentamethylrhodocenium Chloride (7b): Starting materials: 2,6-dichloro-*N*-(1-{5-[1-(2,6-dichlorphenyl)amino-1-phenylmethylene]-cyclopenta-1,3-dien-1-yl}-1-phenylmethylene)aniline (**3b**) (287 mg, 0.51 mmol) and $[Cp^*RhCl_2]_2$ (150 mg, 0.24 mmol). Yield: 272 mg (67%). ^{1}H NMR (300 MHz, CD_2Cl_2, 298 K): δ = 2.19 (s, 15 H, Cp*CH_3), 5.31 (t, 1 H, Cp*H*), 5.94 (d, 2 H, Cp*H*), 6.65, 6.81, 6.83, 6.86, 7.05, 7.08, 7.11–7.13, 7.16, 7.19 (16 H, Ph*H*) ppm. ^{13}C NMR (300 MHz, CD_2Cl_2, 298 K): δ = 11.2 (Cp*CH_3), 90.8 [d, $^1J(^{103}Rh\text{-}^{13}C)$ = 6.4 Hz, Cp], 91.9 [d, $^1J(^{103}Rh\text{-}^{13}C)$ = 6.5 Hz, Cp], 103.8 [d, $^1J(^{103}Rh\text{-}^{13}C)$ = 8.0 Hz, Cp*], 104.1 [d, $^1J(^{103}Rh\text{-}^{13}C)$ = 6.5 Hz, Cp], 124.1, 124.7, 125.2, 127.7, 128.0, 128.3, 128.9, 130.7, 131.1, 135.2 (Ph), 166.4 (*C*=N) ppm. MS (FAB pos): *m*/*z* = 798.87 (M^+ of cation). IR (ATR): $\tilde{\nu}$ = 694 (s), 725 (s), 745 (s), 768 (s), 789 (s), 885 (m), 956 (w), 1023 (s), 1067 (m), 1228 (w), 1259 (s), 1343 (w), 1375 (w), 1427 (s), 1459 (w), 1548 (m), 1579 (w), 1615 (m, C=N), 1722 (w), 1735 (w), 2848 (w), 2914 (w), 2959 (w), 3061 (w) cm^{-1}. $C_{45}H_{42}Cl_5N_2Rh$ (891.02): calcd. C 60.66, H 4.75, N 3.14; found C 60.89, H 4.78, N 3.11.

1′,2′,3′,4′,5′-Pentamethyl-1,3-bis[2,2,2-trifluoro-1-(phenylimino)ethyl]rhodocenium Chloride (8a): Starting materials: *N*-(2,2,2-trifluoro-1-{5-[2,2,2-trifluoro-1-(phenylamino)ethylene]cyclopenta-1,3-dien-2-yl}ethylene)aniline (**4a**) (212 mg, 0.52 mmol) and $[Cp^*RhCl_2]_2$ (160 mg, 0.26 mmol). Yield: 143 mg (40%). ^{1}H NMR (300 MHz, CD_2Cl_2, 298 K): δ = 2.01 (br. s, 15 H, Cp*CH_3), 6.71–6.76 (br. m, 2 H, Cp*H*), 6.83–6.87 (br. m, 1 H, Cp*H*), 7.16–7.51 (br. m, 10 H, Ph*H*) ppm. ^{13}C NMR (300 MHz, CD_3CN, 298 K): δ = 10.5 (br., Cp*CH_3), 89.6 (br., Cp), 95.9 (br., Cp), 104.6 (br., Cp), 115.8, 117.0, 119.3, 122.7, 126.1, 126.5, 129.5, 129.7, 129.9, 130.8, 148.5 (br., Ph) ppm. MS (FAB pos): *m*/*z* = 645.13 (M^+ of cation). IR (ATR): $\tilde{\nu}$ = 694 (s), 765 (s), 872 (w), 987 (w), 1023 (m), 1129 (s), 1165 (s), 1250 (w), 1375 (w), 1446 (m), 1468 (m), 1486 (m), 1592 (s), 1646 (m, C=N), 2852 (w), 2914 (w), 2963 (w), 3373 (w) cm^{-1}. $C_{31}H_{28}ClF_6N_2Rh$ (680.93): calcd. C 54.68, H 4.14, N 4.11; found C 54.79, H 4.17, N 4.08.

1,3-Bis{1-[(2,6-dichlorophenyl)imino]-2,2,2-trifluoroethyl}-1′,2′,3′,4′,5′-pentamethylrhodocenium Chloride (8b): Starting materials: *N*-[2,2,2-trifluoro-1-(5-{2,2,2-trifluoro-1-[(2,6-dichlorophenyl)amino]-ethylene}cyclopenta-1,3-dien-2-yl)ethylene]-2,6-dichloroaniline (**4b**) (464 mg, 0.85 mmol) and $[Cp^*RhCl_2]_2$ (250 mg, 0.40 mmol). Yield: 507 mg (77%). ^{1}H NMR [300 MHz, $CD_3S(O)CD_3$, 313 K]: δ = 2.0 (br. s, 15 H, Cp*CH_3), 5.30 (s, 1 H, Cp*H*), 5.72 (s, 1 H, Cp*H*), 6.29 (s, 1 H, Cp*H*), 6.99 (t, 2 H, Ph*H*), 7.35 (d, 4 H, Ph*H*), 7.61 (t, 2 H, Ph*H*) ppm. ^{13}C NMR (300 MHz, $CDCl_3$, 298 K): δ = 10.0–11.2 (br., Cp*CH_3), 87.5 (br., Cp), 90.9 (br., Cp), 97.6 (br., Cp), 103.6 (br., Cp), 115.9, 116.0, 121.8, 122.9, 125.2, 127.4, 128.1, 129.1, 129.4, 131.2, 135.2, 142.3, 147.0 (Ph), 169.1 (*C*=N) ppm. MS (FAB pos): *m*/*z* = 782.75 (M^+ of cation). IR (ATR): $\tilde{\nu}$ = 717 (m), 739 (s), 771 (s), 787 (s), 872 (m), 987 (m), 1027 (m), 1063 (m), 1085 (m), 1133 (s), 1170 (m), 1232 (w), 1259 (w), 1294 (w), 1357 (w), 1375 (w), 1432 (s), 1481 (m), 1584 (m), 1619 (m, C=N), 2914 (w), 2954 (w) cm^{-1}. $C_{31}H_{24}Cl_5F_6N_2Rh$ (818.71): calcd. C 45.48, H 2.95, N 3.42; found C 45.40, H 2.98, N 3.39.

Electrochemistry: The electrochemical work was performed with a BAS CV50 potentiostat in a custom-made vacuum-tight one-compartment cell that used a 1.6 mm diameter Pt-disk working electrode from BAS, a platinum spiral as the counter electrode, and a silver spiral as a pseudoreference electrode. Each of the spiral-shaped electrodes was welded to Vycon wire and sealed into a glass tube. The counter and reference electrodes were introduced into the cell by appropriate fittings in the side-wall and were sealed by using a Quickfit screw. The potential calibration was performed by adding an appropriate amount of ferrocene or decamethylferrocene ($E_{1/2}$ = –0.55 V vs. ferrocene) to the analyte solution and then re-

Table 2. Crystallographic data for **5a**, **6b**, and **7a**.

Compound	**5a**	**6b**	**7a**
Empirical formula	$C_{29}H_{28}ClO_2Rh{\cdot}4H_2O$	$C_{56}H_{55}BNORh{\cdot}CH_2Cl_2$	$C_{45}H_{46}ClN_2Rh{\cdot}1.5CH_2Cl_2$
M	618.94	956.66	880.59
Crystal system	monoclinic	orthorhombic	triclinic
Space group	$P2_1/c$	*Pbcn*	$P\bar{1}$
a [Å]	16.3853(2)	41.9474(8)	11.2946(3)
b [Å]	11.8272(2)	12.1687(2)	13.9477(3)
c [Å]	14.9842(3)	19.4506(4)	28.8910(5)
α [°]	90	90	90.857(1)
β [°]	99.093(1)	90	95.315(1)
γ [°]	90	90	100.546(1)
Z	4	8	4
V [Å^3]	2867.33(8)	9928.5(3)	4452.82(17)
T [K]	233(2)	233(2)	233(2)
θ range [°]	2.1–27.5	2.1–25.0	1.5–24.0
Data	22472	34200	21714
Unique data	6555	8280	13465
R_{int}	0.0203	0.0309	0.0324
R_1	0.0245	0.0377	0.0768
wR_2	0.0595	0.0881	0.2119
Parameters	371	594	1051
GooF	1.040	1.027	1.032
Peak/hole [e/Å^3]	0.327/–0.414	0.340/–0.398	1.044/–0.763

peating all of the necessary scans that were previously performed on the pure analyte in the presence of the standard. The cooling was performed by immersing the cell into a Dewar vessel that had been cooled with a 2-propanol/dry ice slush bath and allowing thermal equilibration to take place for at least 30 min. The electrodes were polished with diamond paste, 1 μm and 0.2 μm, on the appropriate polishing cloths from Wirtz & Bühler.

X-ray Crystallography: The single-crystal X-ray measurements and structure determinations for **5a**, **6b**, and **7a** (Table 2, Figures 1, 2, and 3) were performed as described below. The data collection was performed with a Nonius Kappa CCD diffractometer that was equipped with graphite-monochromatized Mo-K_α-radiation (λ = 0.71073 Å) and a nominal crystal-to-area detector distance of 36 mm. The intensities were integrated by using DENZO and were scaled with SCALEPACK.[19] Several scans were made in the ϕ- and ω-directions in order to increase the number of redundant reflections, which were averaged in the refinement cycles. This procedure replaced an empirical absorption correction. The structures were solved with direct methods (SHELXS-86) and were refined against F^2 (SHELX-97).[20] The hydrogen atoms at the carbon atoms were added geometrically and were refined by using a riding model. All of the non-hydrogen atoms were refined with anisotropic displacement parameters. **7a** crystallizes with two molecules in the asymmetric unit, and the high R value was probably caused by position disordering of the solvent molecules and the two chlorine anions, which are split over four positions. The high anisotropic displacement factors for all of the atoms showed that the major molecules are also slightly disordered. CCDC-791688 (for **5a**), -791689 (for **6b**), and -791690 (for **7a**) contain the supplementary crystallographic data for this paper. These data can be obtained free of charge from The Cambridge Crystallographic Data Centre via www.ccdc.cam.ac.uk/data_request/cif.

Supporting Information (see footnote on the first page of this article): Electrochemical Figures S1–S7.

[1] a) G. Wilkinson, *J. Am. Chem. Soc.* **1952**, *74*, 6148; b) E. O. Fischer, W. Pfab, *Z. Naturforsch. B* **1952**, *7*, 377; c) E. O. Fischer, R. Jira, *Z. Naturforsch. B* **1953**, *8*, 1.

[2] a) F. A. Cotton, R. O. Whipple, G. Wilkinson, *J. Am. Chem. Soc.* **1953**, *75*, 3586; b) R. J. Angelici, E. O. Fischer, *J. Am. Chem. Soc.* **1963**, *85*, 3733.

[3] E. O. Fischer, U. Zahn, *Chem. Ber.* **1959**, *92*, 1624.

[4] a) T. J. Kealy, P. L. Pauson, *Nature* **1951**, *168*, 1039; b) S. A. Miller, J. A. Tebboth, J. F. Tremaine, *J. Chem. Soc.* **1952**, 632; c) Review on the history of the discovery of ferrocene: P. Laszlo, R. Hoffmann, *Angew. Chem.* **2000**, *112*, 127; *Angew. Chem. Int. Ed.* **2000**, *39*, 123.

[5] SciFinder® literature search based on substructure Cp_2M (M = Fe^{II}) and Cp_2M^+ (M = Co^{III}, Rh^{III}, Ir^{III}).

[6] a) B. Enk, H. Kopacka, K. Wurst, T. Müller, B. Bildstein, *Organometallics* **2009**, *28*, 5575; b) B. Enk, D. Eisenstecken, H. Kopacka, K. Wurst, T. Müller, F. Pevny, R. F. Winter, B. Bildstein, *Organometallics* **2010**, *29*, 3169.

[7] a) J. E. Sheats, W. C. Spink, R. A. Nabinger, D. Nicol, G. Hlatky, *J. Organomet. Chem.* **1983**, *251*, 93; b) A. Philippopoulos, N. Hadjiliadis, C. E. Hart, B. Donnadieu, P. Mc Gowan, R. Poilblanc, *Inorg. Chem.* **1997**, *36*, 1842.

[8] a) W. J. Linn, W. H. Sharkey, *J. Am. Chem. Soc.* **1957**, *79*, 4970; b) D. Lloyd, N. W. Preston, *J. Chem. Soc. C* **1969**, 2464; c) B. Enk, B. Bildstein, K. Wurst, *Z. Kristallogr., New Cryst. Struct.* **2009**, *224*, 544.

[9] U. Kölle, B. Fuss, *Chem. Ber.* **1984**, *117*, 743.

[10] C. E. Wallace, J. P. Selegue, A. Carillo, *Organometallics* **1998**, *17*, 3390.

[11] A. Solchinger, K. Wurst, H. Kopacka, B. Bildstein, *Cryst. Growth Des.* **2007**, *7*, 2380 and references cited therein.

[12] Reviews: a) J. M. Ernsting, S. Gaemers, C. J. Elsevier, *Magn. Reson. Chem.* **2004**, *42*, 721; b) W. von Philipsborn, *Chem. Soc. Rev.* **1999**, *28*, 95; c) B. E. Mann, "Rhodium-103" in *Studies in Inorganic Chemistry 13: Transition Metal Nuclear Magnetic Resonance* (Ed.: P. S. Pregosin), Elsevier Science Publishers B. V., Amsterdam, **1991**, p. 177; d) R. Benn, A. Rufinska, *Angew. Chem.* **1986**, *98*, 851; *Angew. Chem. Int. Ed. Engl.* **1986**, *25*, 861.

[13] E. Maurer, S. Rieker, M. Schollbach, A. Schwenk, T. Egolf, W. von Philipsborn, *Helv. Chim. Acta* **1982**, *65*, 26.

[14] The chemical shift value of $Cp_2Rh^+Cl^-$ versus external $Rh(acac)_3$ was calculated by comparing the published values for [Rh(acac)cod] against $Rh(acac)_3$[12c] and against the commonly used ^{103}Rh reference frequency Ξ = 3.16 MHz:[12] [δ{Rh(acac)cod} = –7014 ppm[12c] – (+1294.2) ppm[13] = –8308 ppm]; [$\delta(Cp_2Rh^+Cl^-)$ = –8308 ppm – 1838.7 ppm[13] = –10147 ppm].

[15] E. O. Fischer, H. Wawersik, *J. Organomet. Chem.* **1966**, *5*, 559.

[16] N. El Murr, J. E. Sheats, W. E. Geiger, J. D. L. Holloway, *Inorg. Chem.* **1979**, *18*, 1443.

[17] O. V. Gusev, L. I. Denisovich, M. G. Peterleitner, A. Z. Rubezhov, N. A. Ustynyuk, P. M. Maitlis, *J. Organomet. Chem.* **1993**, *452*, 219.

[18] N. G. Connelly, W. E. Geiger, *Chem. Rev.* **1996**, *96*, 877.

[19] Z. Otwinowski, W. Minor, *Methods Enzymol.* **1997**, *276*, 307.

[20] G. M. Sheldrick, *SHELXTL V.5.1*, Bruker Analytical X-ray Instruments Inc, Madison, USA, **1997**.

Received: March 4, 2011
Published Online: May 25, 2011

